Ocean Dynamics (2005) 55: 458–475
DOI 10.1007/s10236-005-0033-2

Tal Ezer · Deeptha V. Thattai · Björn Kjerfve
William D. Heyman

On the variability of the flow along the Meso-American Barrier Reef system: a numerical model study of the influence of the Caribbean current and eddies

Received: 27 January 2005 / Accepted: 31 August 2005 / Published online: 11 October 2005

Abstract A high resolution (3–8 km grid), 3D numerical ocean model of the West Caribbean Sea (WCS) is used to investigate the variability and the forcing of flows near the Meso-American Barrier Reef System (MBRS) which runs along the coasts of Mexico, Belize, Guatemala and Honduras. Mesoscale variations in velocity and temperature along the reef were found in seasonal model simulations and in observations; these variations are associated with meandering of the Caribbean current (CC) and the propagation of Caribbean eddies. Diagnostic calculations and a simple assimilation technique are combined to infer the dynamically adjusted flow associated with particular eddies. The results demonstrate that when a cyclonic eddy (negative sea surface height anomaly (SSHA)) is found near the MBRS the CC shifts offshore, the cyclonic circulation in the Gulf of Honduras (GOH) intensifies, and a strong southward flow results along the reef. However, when an anticyclonic eddy (positive SSHA) is found near the reef, the CC moves onshore and the flow is predominantly westward across the reef. The model results help to explain how drifters are able to propagate in a direction opposite to the mean circulation when eddies cause a reversal of the coastal circulation. The effect of including the Meso-American Lagoon west of the Belize Reef in the model topography was also investigated, to show the importance of having accurate coastal topography in determining the variations of transports across the MBRS. The variations found in transports across the MBRS (on seasonal and mesoscale time scales) may have important consequences for biological activities along the reef such as spawning aggregations; better understanding the nature of these variations will help ongoing efforts in coral reef conservation and maintaining the health of the ecosystem in the region.

Keywords West Caribbean Sea · Caribbean eddies · Meso-American Barrier Reef · Numerical model

Responsible Editor: Alejandro Souza

T. Ezer (✉)
Atmospheric and Oceanic Sciences,
Princeton University, Princeton, NJ 08544-0710, USA
E-mail: ezer@splash.princeton.edu
Tel.: +1-609-2581318
Fax: +1-609-2582850

D. V. Thattai
SRM Institute of Science and Technology, Deemed University,
Kattankulathur, India

B. Kjerfve · W. D. Heyman
College of Geosciences, Texas AM University,
College Station, TX 77843, USA

1 Introduction

The West Caribbean Sea (WCS) between 15–22°N and 76–87°W plays an important role in the route of the subtropical gyre circulation, connecting the Caribbean current (CC) with the Loop current (LC) of the Gulf of Mexico; after passing through the Straits of Florida and Cape Hatteras, the current becomes part of the Gulf Stream (Fig. 1). The WCS is open to the Caribbean Sea in the southeast and to the Gulf of Mexico through the Yucatan Channel in the northwest. The Cayman Basin that lies between the Nicaragua Rise and the Cayman Ridge has depths of more than 5,000 m. The strong change in bathymetry is an important factor in the modification of eddies that pass through the WCS (Molinari et al. 1981; Sou et al. 1996). In the western portion of the WCS the Meso-American Barrier Reef System (MBRS) is found; the MBRS is the longest barrier reef in the Western Hemisphere (and the second longest in the world), stretching for more than 1,000 km along the coasts of Mexico, Belize, Guatemala and Honduras. The MBRS is an ecologically and biologically sensitive region that plays an important role in the economy of the surrounding countries (fishing, tourism, etc.). Therefore, a number of marine reserves have been established in the region (Heyman and Kjerfve 2000; Roberts et al. 2002; Appeldoorn and Lindeman 2003; Burke and Maidens 2004; Gibson et al. 2004). Of a

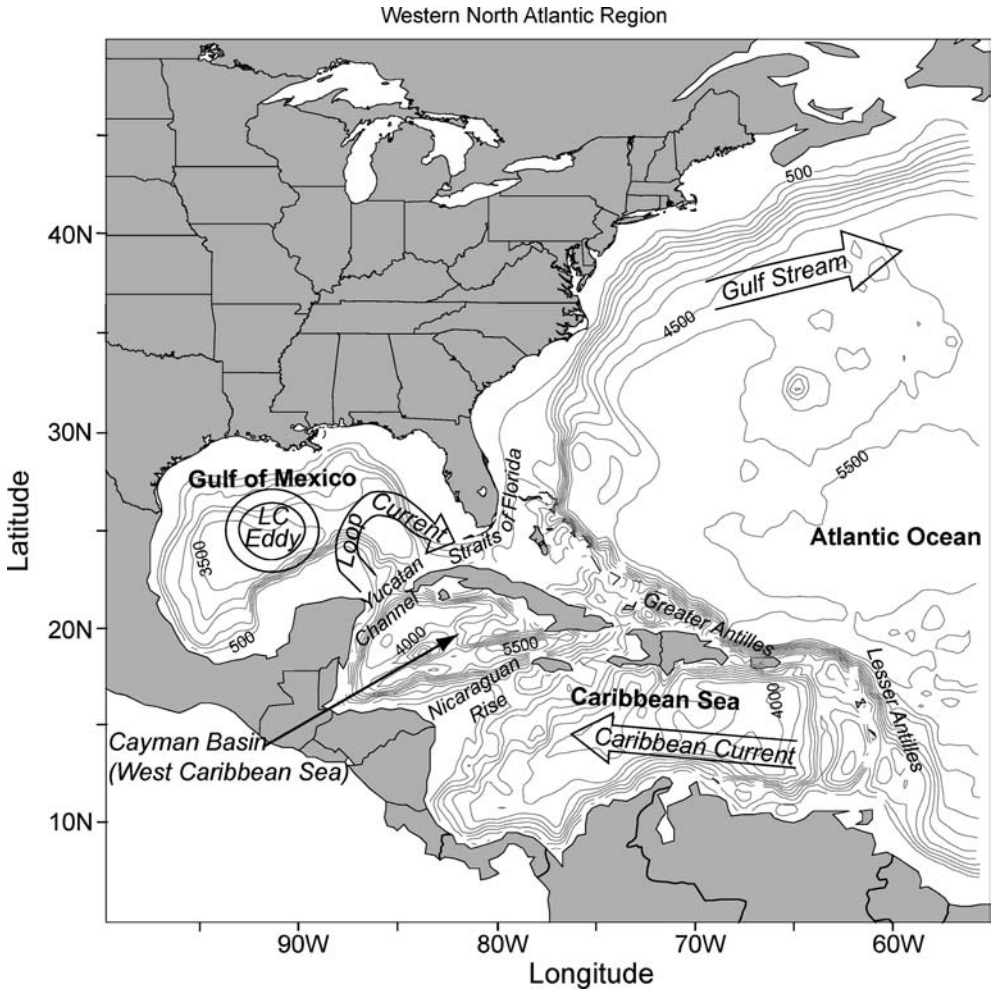

Fig. 1 Topographic map (with depth contours in meters) of the western North Atlantic Ocean and the maior currents and features of the region. The area of interest of this study, the WCS, is indicated by the *arrow*

particular interest is the recent discovery of major spawning aggregation sites for various species of fish in this area (Heyman et al. 2001, 2005; Sala et al. 2001). The health of the reef is also affected by climatic changes that may have already caused significant coral decline and bleaching in the Caribbean Sea (Aronson et al. 2002; Gardner et al. 2003) and by potential pollution of river runoffs due to expanding agriculture and industry in the region (Thattai et al. 2003). For scientific, monitoring and management purposes one needs to understand the variability and forcing influencing the flow near the MBRS, but unfortunately, the region is lacking long-term measurements of currents, especially around the Gulf of Honduras (GOH) and the coast of Belize.

Of the few available historical data in the region two examples are shown in Fig. 2. Figure 2a (from Craig's 1966 book on fishing in British Honduras- before it became Belize; www.ambergriscaye.com/pages/mayan/geographyoffishing.html) composed various current observations to describe a north-westward offshore flow of the CC (which is also called the Yucatan Current in its northern portion), southward flow along the Belize Reef and the Meso-American Lagoon and a cyclonic circulation in the GOH. Figure 2b shows the track of two drifters at 15 m depth from the World Ocean Circulation Experiment (WOCE) data set (see Frantentoni 2001, for analysis of those drifters in the entire North Atlantic). The drifter deployed in the southern part of the reef (east of Sapodilla Cays) moved south and then eastward, following the cyclonic gyre seen in Fig. 2a. The other drifter, deployed further north (west of Glover's Reef), moved north (~200 km in 20 days). Note however, that the latter drifter indicates a northward velocity from Glover's Reef and through the passage between Turneffe Islands Atoll and Lighthouse Reef which is in a direction opposite to the southward flow west of Lighthouse Reef shown in Fig. 2a. The reason for the contradiction between Fig. 2a and b may indicate a change in flow due to seasonal changes, wind or mesoscale variability. However, model results (discussed later) strongly suggest that mesoscale variations during the launching time of the drifters can explain their behavior.

With limited observations in the regions, numerical ocean models may be useful tools to study the flow variability in the region. Of particular interest is to study how the MBRS is influenced by Caribbean Sea circulation changes and eddies. Detailed observations that

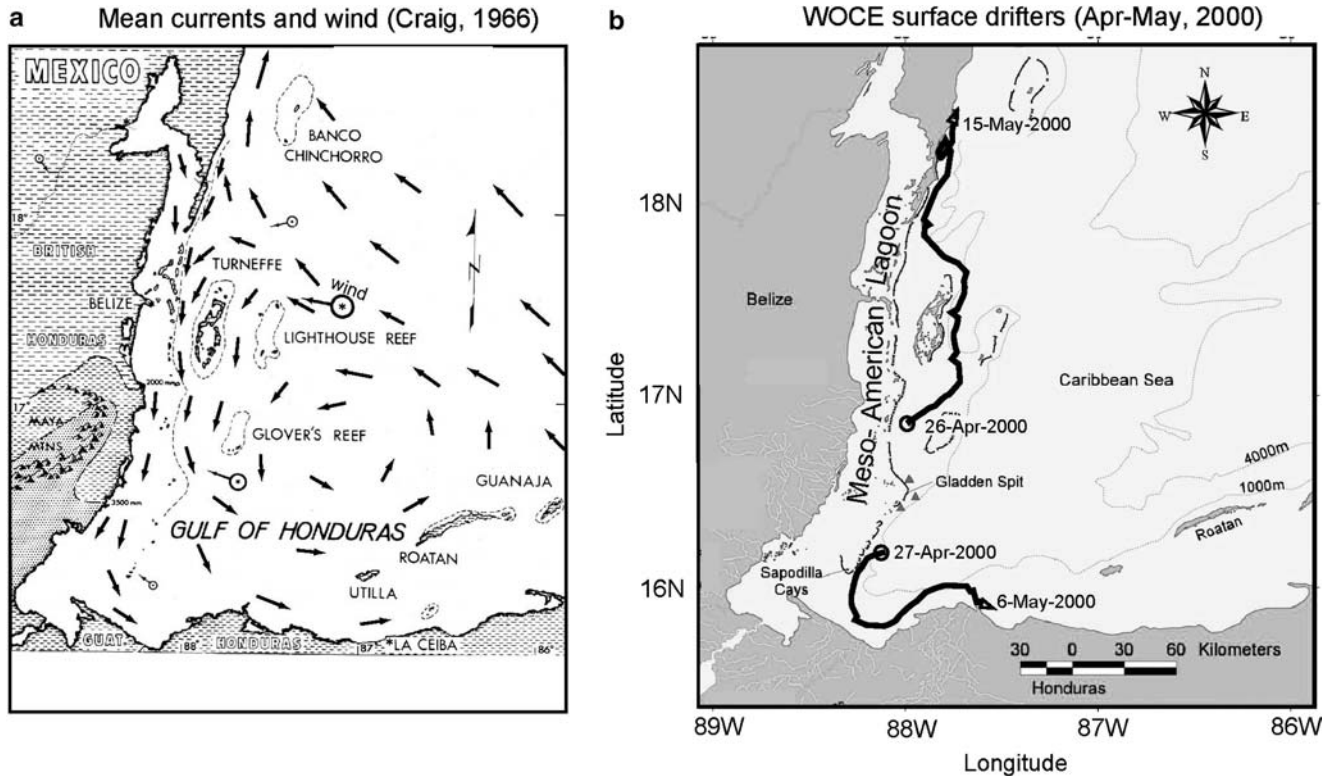

Fig. 2 Observed flow field near the MBRS. **a** Mean currents (*arrows*) and winds (*arrows with circles*) as composed from various observations (based on a larger map from Craig 1966). **b** Two WOCE drifters at 15 m depth (launched on April 2000 at the locations indicated by the *circles*)

show the important interaction between eddies and shelf circulation have been done in regions such as the western Gulf of Mexico (Vidal et al. 1992), but not in the WCS. Caribbean eddies have been studied in the past by observations and models (Carton and Chao 1999; Murphy et al. 1999; Andrade and Barton 2000; Oey et al. 2003), but their influence on the MBRS is still not clear. In fact, in earlier studies, the CC was described as a steady westward flow from the Lesser Antilles through three major deep-water basins and via the Yucatan Channel into the Gulf of Mexico, with little or no variability in the western portion of the Caribbean Sea (Gordon 1967; Brucks 1971). Later studies indicated the presence of some variability in the western Caribbean but did not describe in any detail the western Caribbean as they focused on the Caribbean Sea in its entirety (Molinari et al. 1981; Kinder et al. 1983; Carton and Chao 1999; Andrade and Barton 2000). Sou et al. (1996) applied a numerical model to the Caribbean and simulated the presence of gyres near the GOH. Murphy et al. (1999) in their model study focused on the eddy connectivity in the Intra-America Seas. They simulated the formation of mesoscale eddies in the Lesser Antilles and tracked the translation of the eddies in the Caribbean Sea and through the Yucatan Channel. Their model showed greater detail in the Lesser Antilles region but not in the GOH. The minimum depth in the model was 200 m, which excludes the continental shelves. In recent years various realistic models of the Caribbean Sea and the Gulf of Mexico have been developed for scientific and prediction purposes (Candela et al. 2003; Morey et al. 2003; Ezer et al. 2003; Oey et al. 2003; Romanou et al. 2004; Sheng and Tang 2003, 2004). For a review of numerical models of the region see Oey et al. (2005). Nevertheless, of all the above models only Sheng and Tang's model focuses on the WCS and the MBRS, first using a coarse resolution (~20 km) model of the WCS (2003 paper) and then using a nested grid (~6 km; 2004 paper) for the MBRS region. Their *z*-level model simulated well the mean circulation (including the cyclonic circulation in the GOH) and the seasonal variations; they show that the circulation near the MBRS is not too sensitive to climatological wind, but is very sensitive to model density and open boundary conditions. We will repeat here some of their sensitivity experiments using a terrain following (''sigma'') model (the Princeton Ocean Model, POM), but with a higher resolution grid that better captures the detailed coastal topography near the coast of Belize; we will also examine the direct effect of mesoscale eddies on the MBRS.

The main objective of the study is to get a better understanding of the variability of the flow along the MBRS and the main forcing mechanisms involved. In particular, the interaction between open ocean circulation (including mesoscale eddies) and the coastal flows near the reef is not well understood, but may be

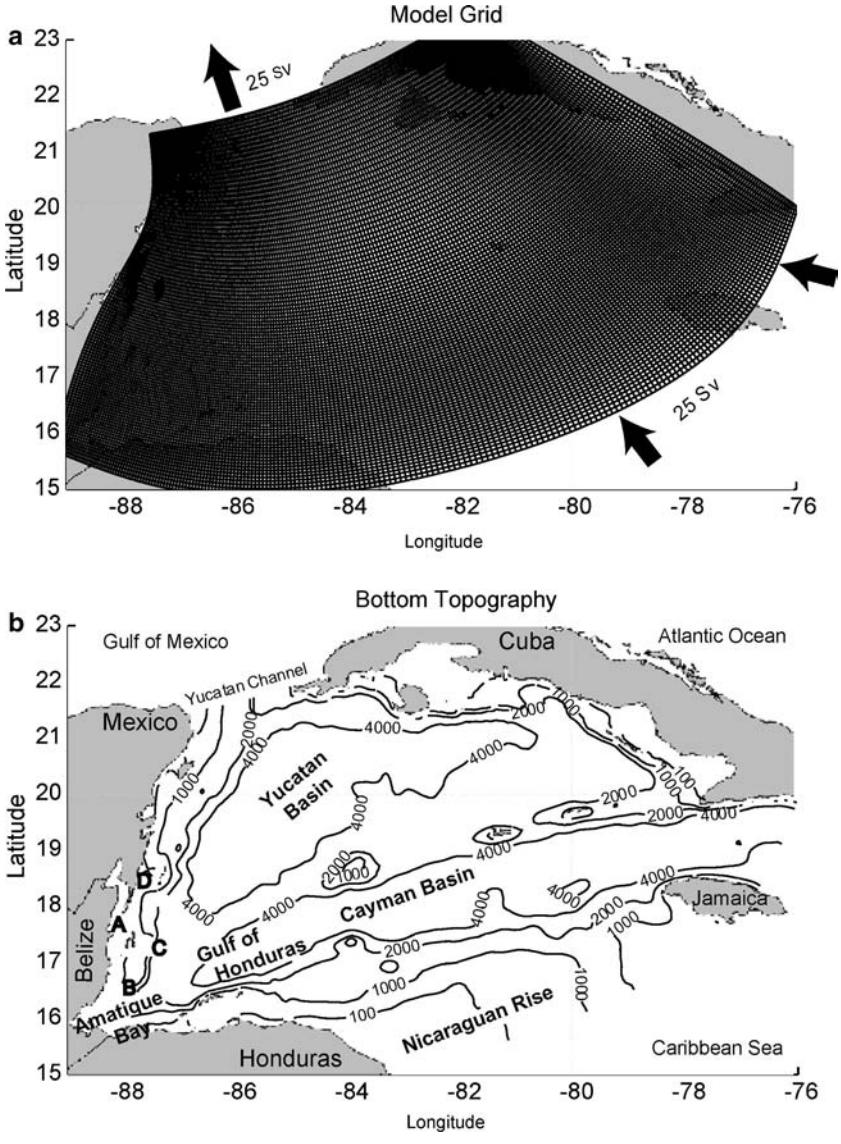

Fig. 3 **a** Curvilinear orthogonal model grid (note that in the model itself land points are masked and not used in the calculations) and **b** bottom topography (depth contours in m). Particular locations where time series are shown are indicated by *A* Meso-American Lagoon, near Belize City, *B* Gladden Spit, *C* Lighthouse Reef and *D* Chinchorro Channel

important here because of the unique topography of the region and the closeness of the MBRS to the deep sea. The paper is organized as follows. First, the model setup is described in Sect. 2. In Sect. 3 results from seasonal and then diagnostic calculations are analyzed, and finally, discussion and conclusions are offered in Sect. 4.

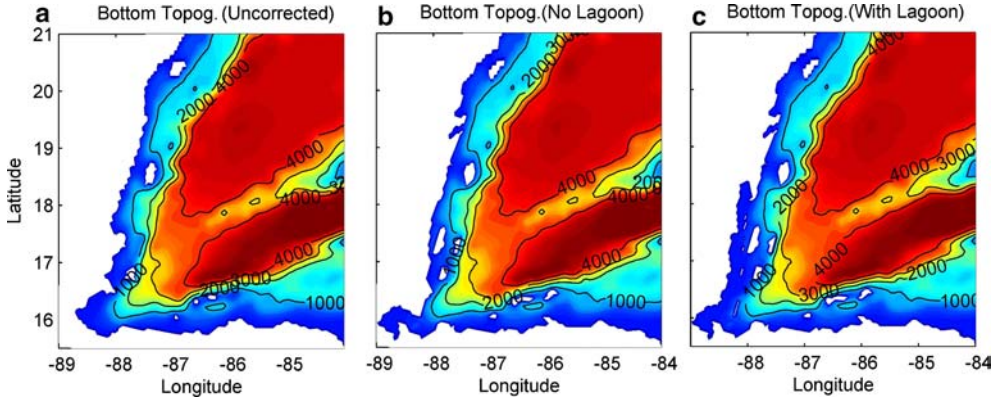

Fig. 4 Zoom on the bottom topography in the MBRS region. **a** Original bathymetry if directly interpolated from the Digital Terrain Model data set without any correction. **b** Bathymetry after manual correction with the western coastal boundary of the model set along the Belize barrier reef. **c** Bathymetry after manual correction where the model grid extends into the Meso-American Lagoon west of the Belize Reef

Table 1 Observed and model harmonics for tides at six stations along the MBRS

	Observed		Model		Difference	
	Amplitude (cm)	Phase (°)	Amplitude (cm)	Phase (°)	Amplitude (cm)	Phase (°)
Puerto Morelos (20°52′N and 86°52′W)						
O1	2.4	347	2.2	333	0.2	14
K1	0.5	254	2.9	268	−2.4	−14
N2	2.5	27	2.1	70	0.4	−43
M2	7.1	52	6.6	52	0.6	0
S2	2.6	44	2.4	24	0.2	20
Lighthouse (17°26′N and 87°26′W)						
O1	2.2	346	2.3	334	−0.1	13
K1	1.9	268	2.8	267	−0.9	1
N2	2.2	67	2.2	70	0	−3
M2	6.5	84	6.8	82	−0.3	2
S2	2.8	50	2.2	27	0.6	23
Belize City (17°28′N and 88°12′W)						
O1	3.2	332	2.4	333	0.8	−1
K1	2.3	279	2.8	268	−0.5	11
N2	3.5	76	2.2	70	1.3	6
M2	8.0	84	6.8	82	1.2	2
S2	3.2	36	2.3	27	0.9	9
Gladden (16°32′N and 87°59′W)						
O1	2.4	331	2.3	334	0.1	−3
K1	2.7	281	2.9	269	−0.2	12
N2	2.3	61	2.2	71	0.1	−10
M2	5.8	87	7.1	91	−1.3	−4
S2	3.0	49	2.3	29	0.7	20
Sapodilla (16°9′N and 89°14′W)						
O1	2.3	326	2.3	335	0	−9
K1	2.8	262	2.8	268	0	−6
N2	2.4	71	2.2	70	0.2	1
M2	6.1	88	7.2	94	−1.1	−6
S2	2.7	54	2.4	24	0.3	30
Puerto Cortes (15°50′N and 87°57′W)						
O1	2.5	327	2.3	335	0.2	−8
K1	2.9	269	2.8	268	0.1	1
N2	2.3	71	2.2	71	0.1	0
M2	5.9	86	7.3	98	−1.4	−12
S2	2.3	24	2.2	29	0.1	−5

2 Model description and setup

The WCS model (described in detail in Thattai 2003) is based on the POM which is a 3D, free surface, primitive equation, finite difference model (Blumberg and Mellor 1987). It is a sigma coordinate (terrain-following) model (see Ezer et al. 2002, for a review of terrain-following ocean models), so the water column is divided into an equal number of proportional vertical layers regardless of the local depth. The transformation from z to σ is defined by $\sigma = (z-\eta)/(H + \eta)$, where η is the surface elevation and H is the water column depth, so that at the surface ($z=\eta$) $\sigma=0$, and at the bottom ($z=-H$) $\sigma = -1$. The horizontal grid uses curvilinear orthogonal coordinates, and a staggered "Arakawa C" numerical grid. The model employs a split time step, with a short time step for the external mode (2D, vertically integrated equations) and a longer time step for the internal mode (3D). In the WCS case the external time step is 6 s and the internal time step is 3 min. The model contains an imbedded second moment turbulence closure scheme to provide vertical mixing coefficients (Mellor and Yamada 1982), and a Smagorinsky-type horizontal mixing (Smagorinsky et al. 1965) which depends on grid size and velocity gradients. The monthly climatological values of T and S, T_{Clim} and S_{Clim}, are subtracted from the temperature and salinity in the diffusion terms which is shown to be an effective way to reduce unwanted diapycnal mixing over steep topography (Mellor and Blumberg 1985; Ezer and Mellor 2000). Area-averaged climatological density $\rho_{\mathrm{Mean}}(x,y,\sigma)=\rho_{\mathrm{obs}}(z)$ is subtracted in the pressure gradient calculations, which is a standard procedure in regional POM applications to significantly reduce pressure gradient errors over steep topography (Mellor et al. 1994, 1998). The general digital environmental model (GDEM, Teague et al. 1990) monthly climatology is used for T_{Clim} and S_{Clim} , as well as for initialization.

The curvilinear model grid for the WCS and the bottom topography are shown in Fig. 3. The grid consists of 20,301 cells with 16 vertical layers. The proportional vertical layers were selected at $\sigma = 0$, -0.002, -0.003, -0.007, -0.014, -0.028, -0.056, -0.111, -0.222, -0.333, -0.444, -0.556, -0.667, -0.778, -0.889 and -1.000 the total local depth. Thus, since temperature, salinity, density and currents vary most in the upper layers of the ocean the emphasis was on resolving well the variability near the surface. The horizontal grid resolution varies from 3 km along the MBRS to 8 km on the open eastern boundary, and the depth ranges from 1 to 6,000 m. The bathymetry was interpolated from a 1/24° Digital Terrain Model (DTM) grid. However, the topography near the coast was found to be very inaccurate (Fig. 4a) and has to be manually edited along the coastlines to match the depths obtained from detailed charts. Accurate bathymetry is a crucial element in physical–biological interaction in this region. For example, many of the passages, reefs and islands that are important fish aggregation sites were missing or significantly distorted in the original bathymetry. Two model topographies were constructed, one where the land boundary was along the Belize Reef (Fig. 4b) and

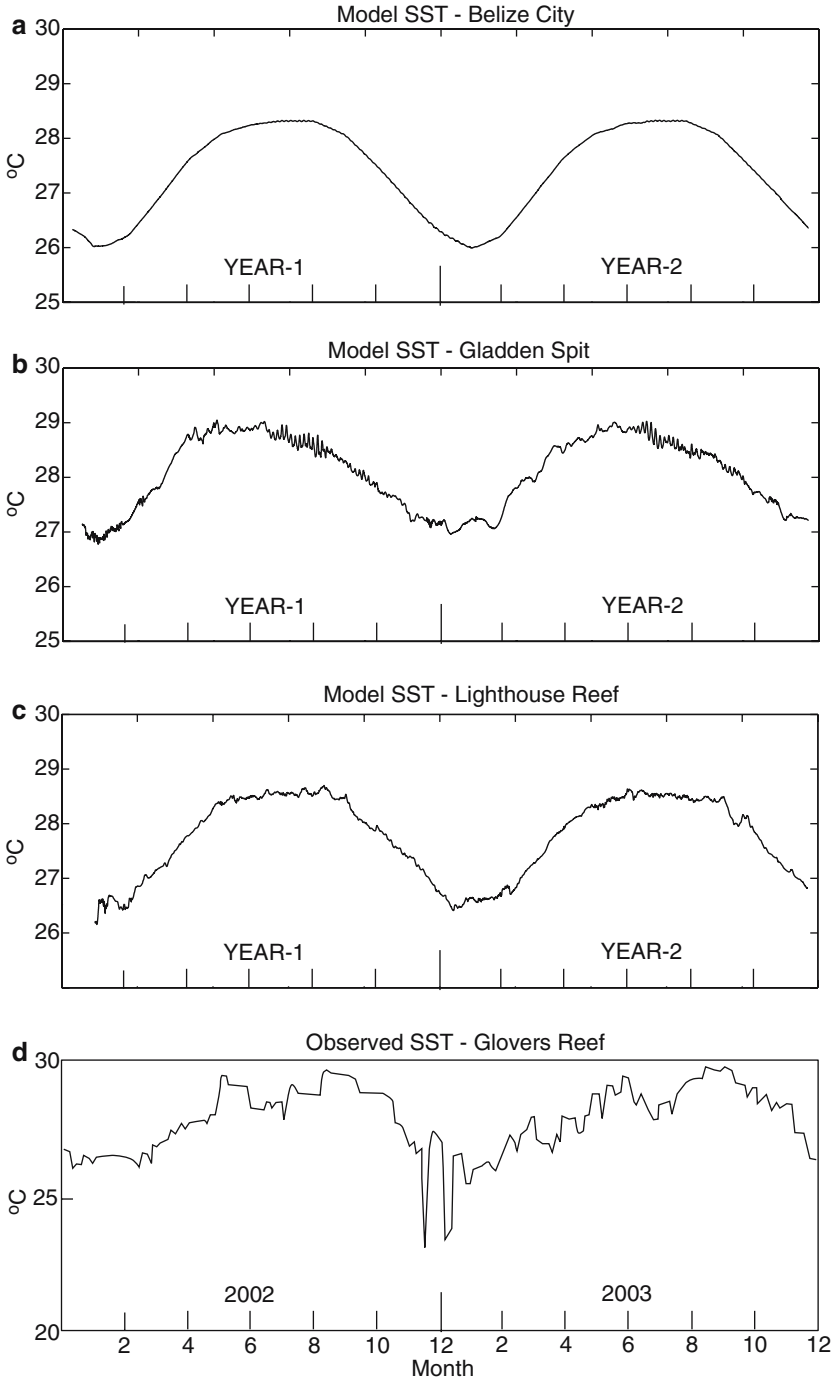

Fig. 5 Examples of 2-years time series of surface temperature. Model calculations with seasonal forcing are shown for **a** Belize City, **b** Gladden Spit, and **c** Lighthouse Reef. Note that **a** is inside the lagoon while **b** and **c** are on the eastern side of the reef (see Fig. 3b for locations). **d** Observed temperature for 2002–2003 from NOAA's Coral Reef Watch (coralreefwatch.noaa.gov), around Glovers Reef (just north of Gladden Spit). Note that the vertical scale in **d** is different than that used in (**a**–**c**)

one where the Meso-American Lagoon west of the reef was included (Fig. 4c). Most experiments use the topography in Fig. 4c, except when indicated otherwise. Note that the model resolution is not fine enough to resolve the details of the lagoon and many small reef channels connecting the lagoon to the open ocean (compared for example with the finite element lagoon-only model of Thattai 2003), but it may provide useful information for the general flow pattern. Surface forcing uses the monthly-mean climatology of wind stress data from the Comprehensive Ocean–Atmosphere Data Set (COADS). The monthly mean wind is generally from east to west (as seen also in Fig. 2a) with only small spatial variations and small changes from one month to another.

A transport of 25 Sv (1 Sverdrup $= 10^6$ m^3 s^{-1}) of the CC is allowed to enter the model in the south and exit into the Gulf of Mexico through the Yucatan Channel in the north; this transport is close to the observed estimates (Ochoa et al. 2001; Bunge et al. 2002; Candela et al. 2003). The model requires open boundary conditions for the external (2D, vertically integrated) and internal (3D) velocities. The external velocities along the open boundaries are interpolated from the annual mean flow of the North Atlantic model of Ezer and Mellor (2000), giving total inflow and outflow transports of 25 Sv each. The internal velocities on the boundaries use a radiation condition. Monthly mean temperature and salinity data are used as lateral boundary conditions and as surface boundary conditions with relaxation to climatology at buffer zones near the boundaries. The surface and lateral boundary conditions are quite similar to the set-up of the Sheng and Tang (2003, 2004) WCS model.

Tidal amplitudes and phases of six constituents (M2, S2, N2, O1, K1, and P1) for the two boundaries were included from data based on Ray's (1999) global model. However, global tidal models are often not very accurate near the coast, so regional models may require some adjustment in the boundary conditions either by optimization or manually (e.g., Chen and Mellor 1999; Wong et al. 2003). Here, we manually adjusted the open boundary conditions to better fit the tidal observations analyzed by Kjerfve (1981). Table 1 compares the model and observed tides at several locations (after the adjustment). The tides in the WCS are relatively small (amplitude of M2 is ~6–8 cm and total amplitude ~10–15 cm) and their contribution to the total surface kinetic energy budget are small compared with wind and mean circulation effects (Thattai 2003). The good agreement between the model and observations (average error of amplitudes ~0.5 cm and of phase ~10°) is not surprising since tidal forcing was adjusted, as described above. Various sensitivity experiments with the WCS model have been conducted in Thattai (2003) using relatively short simulations (order of a few months). Here we perform longer simulations of several years, as well as other sensitivity experiments with diagnostic calculations. We mostly focus on the MBRS and the coastal region near Belize and the GOH, far enough from the direct influence of the open boundary conditions. Nevertheless, allowing the CC to pass through the domain is necessary in order to get the general mean circulation in the model.

3 Results

3.1 Seasonal simulations: flow variability near the reef

Starting from January climatology and forcing the model with monthly wind stress, monthly surface temperature and fixed barotropic transport on the lateral open boundaries, the surface velocity is adjusted within a few weeks and the volume averaged kinetic energy within a few months. Thus, calculations including the spin-up continue for 2 years. The monthly wind over the region changes very little from month to month (mostly westward to southwestward wind vectors) so the only time-dependent high frequency forcing is the tidal forcing (for 1998–1999). It should be noted that the transport boundary conditions in the seasonal simulations do not include the effect of eddies that known to propagate into the WCS from the eastern Caribbean Sea (the effect of eddies will be discussed in Sect. 3.2). The model seasonal changes in surface temperature (with range between 26 and 29°C, largely controlled by the surface monthly climatology) at several locations are shown in Fig. 5a–c. Note that while inside the lagoon (at Belize City, Fig. 5a) only smooth seasonal changes are indicated, near the outside reef (at Gladden Spit and Lighthouse Reef, Fig. 5b, c, respectively) additional

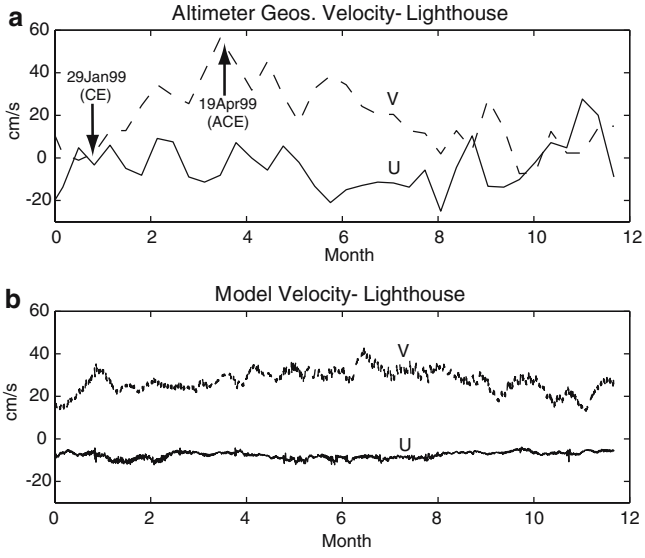

Fig. 6 Time series of surface velocity (east–west, *U* component, in *solid lines* and north–south, *V* component in *dash lines*) near Lighthouse Reef: **a** Geostrophic velocity calculated from Altimeter data during 1999 and **b** velocity calculated by the model with only seasonal surface forcing and tides. The time when a cyclonic eddy (*CE*) and an anticyclonic eddy (*ACE*) were observed near the Gulf of Honduras (*GOH*) are indicated in (**a**)

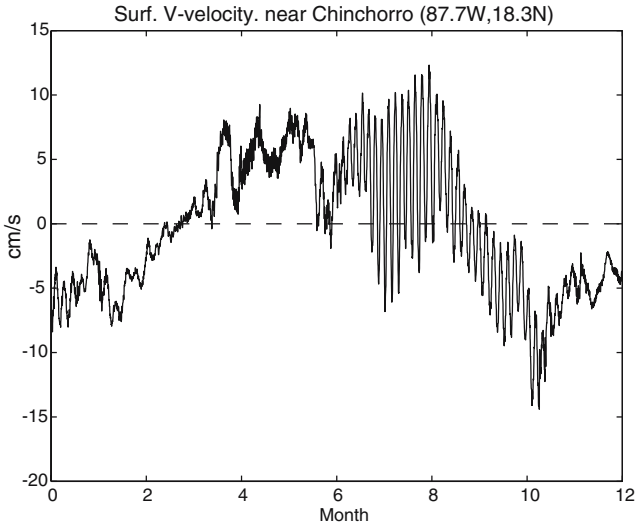

Fig. 7 North–south surface velocity component near the west coast of Chinchorro Channel (see Fig. 3b for location) from the seasonal simulations

small variations (~0.5–1.0°C amplitudes, ~weeks time scales) are evident, even though the model does not have any time-dependent forcing in the mesoscale range (there are, however, some high-frequency tidal-driven variations in Fig. 5b in late summer). Observations (Fig. 5d) from NOAA's Coral Reef Watch program (in Glovers Reef, not far from Gladden Spit) indicate variations in surface temperature with similar time scales but somewhat larger amplitudes (~1–2°C). The observations include, of course, the effects of synoptic atmospheric variations (e.g., the events in December 2002 and January 2003) which are absent from the model. This qualitative comparison at least suggests that there are some variations near the reef which are not associated with direct atmospheric forcing. In fact, analyses of new measurements at several locations along the reef show that the currents are often uncorrelated with the local wind (Armstrong 2005).

Model velocity (second year, Fig. 6b) near Lighthouse Reef shows a persistent north-westward flow (mean $(U,V) \sim ((10, 30)$ cm s^{-1}), but with considerable mesoscale variations (~10–20 cm s^{-1}) in the along-reef component (V); these variations seem to relate to variations in the position of the CC, and are consistent with the diagnostic calculations presented in the next section. To see if such variations are real, the geostrophic velocity was calculated from altimeter data for 1999 (more details on this data set are given in the next section), and the results show very similar mean components as the model, but larger mesoscale variability (Fig. 6a). Note that the altimeter data are from a 1/4°N×1/4°W box on the offshore side of the reef, and represent 10-day composites; so this qualitative data comparison cannot capture the higher frequency oscillations seen in the model hourly data. Since the seasonal simulation is not forced with realistic synoptic winds and does not include data assimilation, direct model data comparisons for particular events are meaningless; the nature of the variations in the model and the data is important though. The hypothesis is that those variations are associated with meandering of the CC and eddies propagating along the reef. Since the idealized model does not explicitly impose eddies or allow them to enter the domain from the south open boundary (as often seen in larger domain models such as in Murphy et al. 1999; Ezer and Mellor 2000; Oey et al. 2003), locally generated variability should be smaller than the observed one, but nevertheless exist.

To investigate the role that Caribbean eddies have on the flow near the reef, two particular days have been chosen (and marked in Fig. 6a)—in the first period (29 January 1999) there is almost zero velocity near the reef, while in the second period (19 April 1999) a strong northward velocity reached 55 cm s^{-1}. These two periods correspond to times when cyclonic and anticyclonic eddies, respectively, were observed near the MBRS (shown later). While the model and the observed flow near Lighthouse Reef (shown in Fig. 6) are northward throughout the year, further north, along the west side of the Chinchorro Channel (Fig. 7), the flow seems to have a seasonal cycle, with a northward flow during the spring and summer (April–September) and a southward flow during the fall and winter months (October–March); this pattern is typical also to other locations in the Chinchorro area and is seen in the first year too. Mesoscale variations (note in particular the April–June period) as well as higher frequency oscillations (July–October) with a period of 4–5 days are also seen in the model. It is interesting to note that though new velocity measurements on the Mexican shelf near Chinchorro (L. Carrillo, personal communication) also indicate high-frequency velocity oscillations that seem to amplify

Table 2 Model topography, initial condition and wind for the diagnostic calculation experiments

Experiment	Topography	Initial condition	Wind forcing
1	With lagoon	January climatology	January climatology
2	With lagoon	April climatology	April climatology
3	With lagoon	29 January 1999 eddies	January climatology
4	With lagoon	19 April 1999 eddies	April climatology
5	No lagoon	29 January 1999 eddies	January climatology
6	No lagoon	19 April 1999 eddies	April climatology
7	With lagoon	April climatology	No wind
8	With lagoon	April climatology	April clim.wind × 2

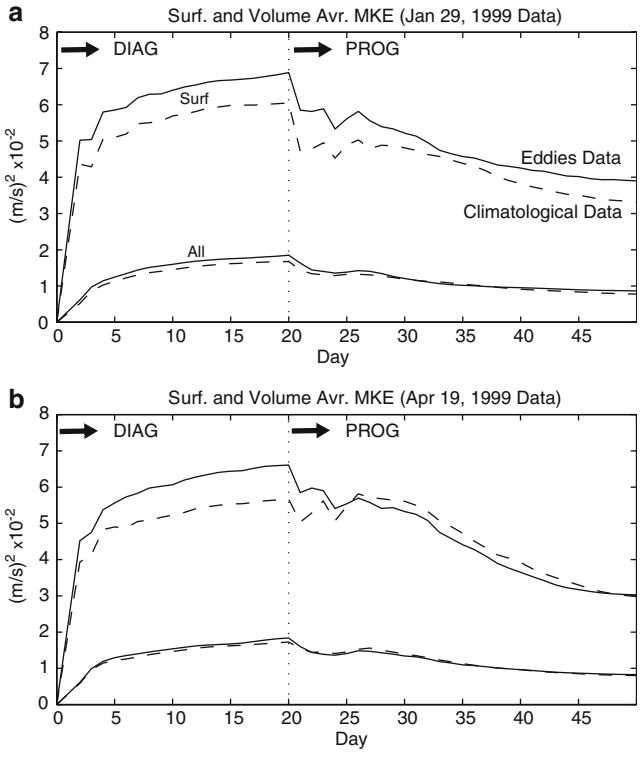

Fig. 8 Mean kinetic energy (*MKE*) for the diagnostic–prognostic calculations: **a** January 1999 and **b** April 1999. *Top lines* in each panel represent the MKE calculated from the average surface velocities, while *bottom lines* are calculations from the volume averaged velocity over the entire water column. Initial density fields are either monthly climatology (*dash lines*) or climatology plus eddies (*solid lines*)

during the summer months and then damped in the fall and winter as indicated by the model. Observations of velocities in the Cozumel Channel near the Yucatan Peninsula (about 200 km north of the Chinchorro Channel) also show fluctuations with periods of 3–7 days that last for a month or more at a time (Ochoa et al. 2005); the authors suggest that these are ageostrophic fluctuations associated with the interaction of the strong current with the Cozumel Island topography. While similar conditions exist for the interaction of the CC with Banco Chinchorro, other mechanisms for these variations cannot be ruled out. For example, at the time of these fluctuations the model indicates some modulation of the tides near Yucatan with 4–5 days period that seem to propagate as a baroclinic wave along the coast. In any case, more research of the origin and mechanism of these interesting oscillations are clearly needed.

The idealized seasonal simulations presented here are not meant to describe the details of the seasonal circulation in the WCS (e.g., see Sheng and Tang 2003) but they point to two interesting results: (1) there are mesoscale variations in flows along the reef even when no such forcing is included in the model, and (2) there is an indication of a seasonal reversal of the flow at some locations along the reef. In the next section, more detailed sensitivity experiments will be used to explain those results.

3.2 Diagnostic calculations: the role of eddies

Diagnostic calculations use the 3D model equations to calculate the dynamically adjusted flow field and sea level for a given topography, density field and wind. This approach usually consists of "pure" diagnostic calculations (holding the density field unchanged), followed by a short prognostic calculation (thus sometimes the approach is called semidiagnostic) with fixed forcing (and often relaxation of model temperatures to observed fields near the surface and the open boundaries). Diffusion and advection processes during the prognostic run help to remove small-scale noise in the velocity field which results from inconsistencies between the observed density field and bottom topography (Ezer and Mellor 1994a). This approach, first introduced by Ezer and Mellor (1994a) to derive the climatological circulation of the North Atlantic, has since been adopted for example, to obtain the circulation associated with local observations in the South China Sea (Wang et al. 2004) and in the Brazil Current (da Silveira et al. 2004).

Model and data time series shown in the previous section suggest that flows near the MBRS may be affected by eddies, so we want to introduce eddies into the model using satellite altimeter data. The altimeter data were obtained from the archiving, validation, and interpretation of satellites oceanographic (AVISO) data set which combines the TOPEX-Poseidon (T/P) and ERS satellite altimeter measurements and provides a complete sea surface height (SSH) anomaly every 10 days on a 1/4°×1/4° grid (Ducet et al. 2000). Following previous assimilation methodology (Mellor and Ezer 1991; Ezer and Mellor 1994b; 1997; Wang et al. 2003), the surface data are interpolated horizontally into the model grid, and then projected vertically into the water column using predetermined surface–subsurface correlations. Thus the "analyzed" temperature T_a derived from the surface SSH anomaly data $\delta\eta$ is obtained from $T_a(x,y,z,t) = T_{Clim}(x,y,z) + F_T(x,y,z)\delta\eta(x,y,t)$. The correlation factor, F_T, is defined by $F_T = <\delta T\delta\eta>/<\delta\eta>^2$, where "$<>$" represent time-averaged terms. This approach, combined with an optimal interpolation scheme, can provide the base for continuous data assimilation (Ezer and Mellor 1994b; Wang et al. 2003). In such cases the correlations are calculated from model statistics based on model simulations of many years. Here, instead, the assimilation is greatly simplified to just introduce an eddy field for a particular day. Based on area-averaged correlations from other models for this region (Ezer and Mellor 2000; Oey et al. 2003) and some empirical trial and error, a simple correlation function $F_T = 6(1 - z/1{,}000\ \text{m})$ is chosen to derive initial condition for the upper 1,000 m. Observations and models (e.g., Carton and Chao 1999) indicate that the signature

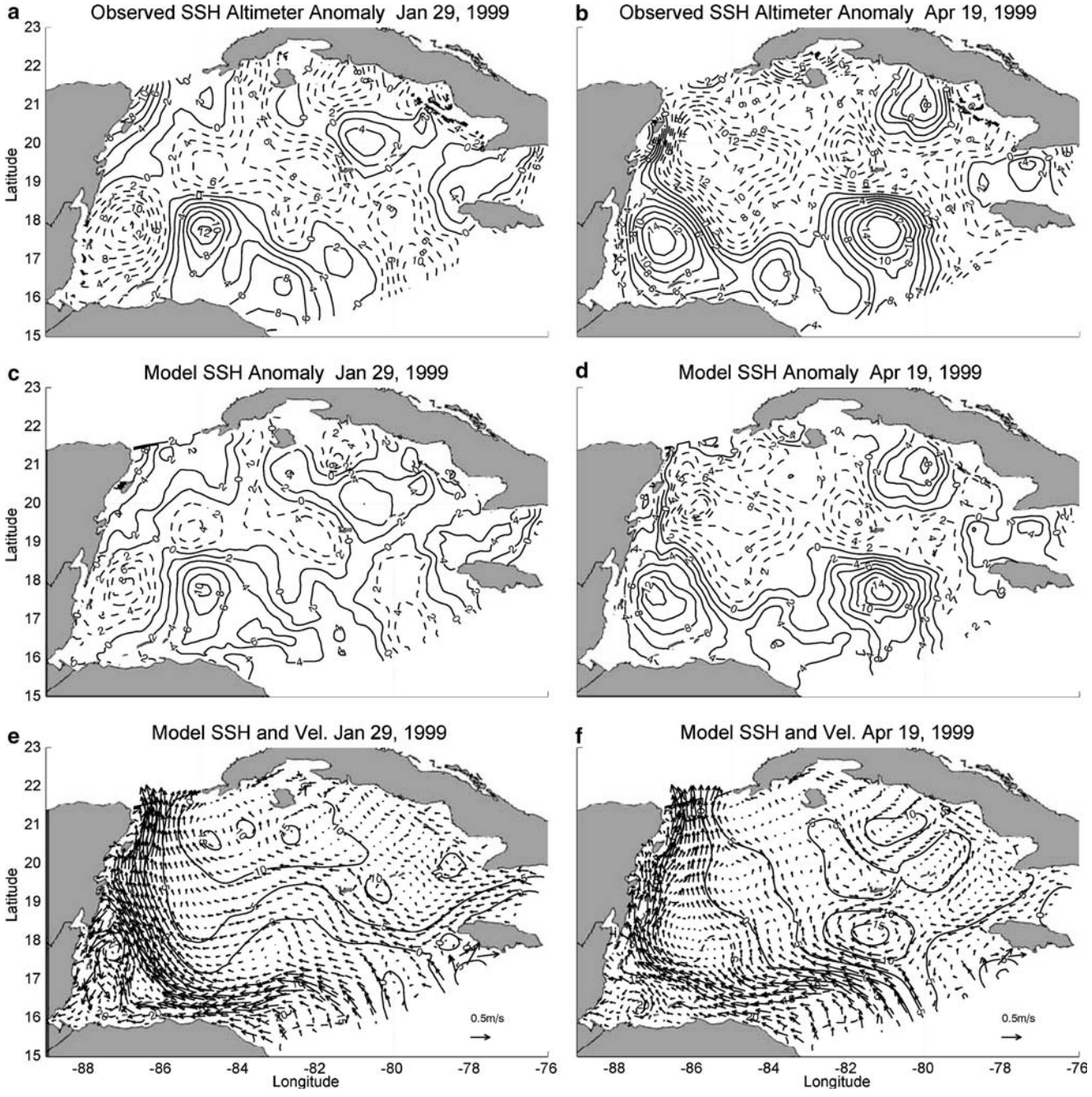

Fig. 9 Sea surface height (*SSH*) anomaly derived from Altimeter data (*top panels*) and from model diagnostic calculations (*middle panels*); contour interval is 2 cm with dash contours for negative (more cyclonic) values. The *bottom panels* are the model absolute SSH (contour interval of 5 cm s^{-1}) and surface velocity vectors after the diagnostic–prognostic adjustment is completed. *Left panels* are for 29 January 1999 and *right panels* are for 19 April 1999

of Caribbean eddies is limited to the upper layers; so below 1,000 m monthly climatology is used. While this approach seems to oversimplify the assimilation, it will be shown that it is sufficient to represent the observed eddies surprisingly well.

Diagnostic calculations of 20 days followed by 30 days of prognostic calculations (which include relaxation of near-surface model temperature to data) are performed for eight different initial conditions, topography and forcing (Table 2). Figure 8 (for experiments 1–4) shows how the model kinetic energy is adjusted during the calculations; after 50 days, a steady state is reached, representing the dynamically adjusted flow field associated with each initial condition and forcing.

Two particular days were chosen to demonstrate the effect of eddies—29 January 1999, when a cyclonic eddy (relative to the mean) was observed in the GOH

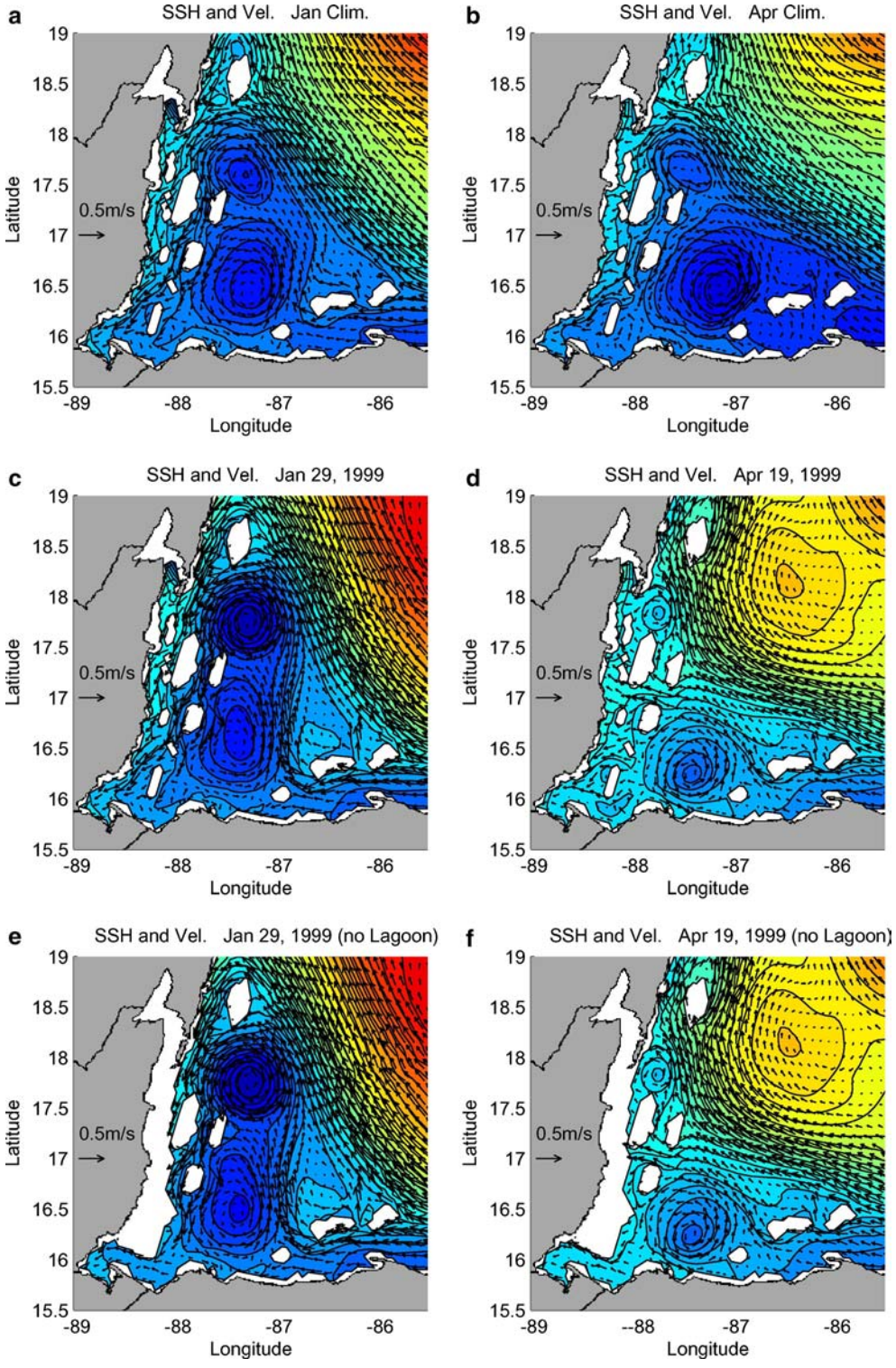

Fig. 10 Sea surface height (in color—high-sea level in *red*, low-sea level in *blue*, maximum range ~30 cm) and surface velocity vectors in the MBRS region from the diagnostic–prognostic calculations. *Top panels* are calculations with monthly climatology, *middle panels* are calculations with eddies and *bottom panels* are calculations with eddies, but without the lagoon topography (Fig. 4b). *Left panels* are for the January case and the *right panels* are for the April case

(in the south-western corner of the domain, Fig. 9a), and—19 April 1999, when an anticyclonic eddy was observed at the same region (Fig. 9b). When initializing the model with temperature field derived from the monthly climatology and observed SSH anomaly as described earlier (monthly wind climatology was also used), the diagnostic calculations reproduced the SSH eddy field very well (comparing Fig. 9a to 9c and Fig. 9b to 9d), which indicates that the assimilation–correlation scheme works well. The total adjusted SSH and surface velocities show a significant shift in the CC, offshore in the January 29 case (Fig. 9e) and onshore in the April 19 case (Fig. 9f).

Figure 10 focuses on the surface flow and circulation in the GOH, showing intensifying cyclonic circulation with strong southward flow over the reef and lagoon on

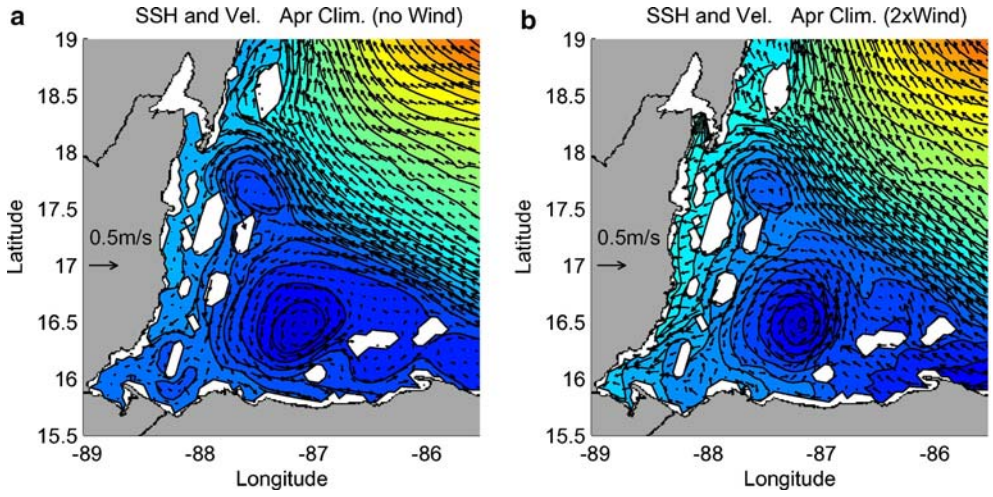

Fig. 11 Same as the April climatology case of Fig. 10b, but for **a** a run with no wind stress, and **b** a run with twice the observed wind stress

January 29 (Fig. 10c) compared with weaker cyclonic circulation and mostly westward flow over the reef on April 19 (Fig. 10d). Note that the onshore shift in the CC during April 19 produces a strong northward flow east of Lighthouse Reef which could explain the data shown in Fig. 6a. To illustrate that the change of flow is due to eddies and not due to differences between January and April climatologies, calculations without eddies are shown in Fig. 10a, b. The climatology has little effect on the general flow with one exception in the Chinchorro channel (north-west corner of the subdomain shown in Fig. 10) where the flow is reversed (southward flow in January and northward flow in April—consistent with the seasonal changes shown in Fig. 7). An explanation for this reversal is given later. If the Meso-American Lagoon is not included in the model topography (Fig. 10e, f) the offshore circulation is unchanged, but westward or southward flows across the reef must return in deeper layers instead of feeding the lagoon. For example, if one is interested in the detailed circulation in the Amatique Bay (south-western most corner of the domain, Fig. 3b), both the model (e.g., Fig. 10c) and observations (Fig. 2a) show that the Bay is fed by transport of water coming from the lagoon in the north and exiting to the east through the Sapodilla Cays. Without the lagoon topography surface inflow and deep outflow in and out of the Bay are through the same opening in the Cays.

The direct influence of the climatological wind is examined using two additional calculations, one with no wind (Fig. 11a) and one with double the observed April monthly wind stress (Fig. 11b). The general offshore circulation is more dominated by the density field and boundary conditions rather than by the local wind, as also shown by Sheng and Tang (2004). However, surface flows are stronger with double winds and in particular the westward wind causes higher sea level along the coast with larger transports across the reef and into the lagoon. More realistic simulations with synoptic winds (now underway) should show a stronger influence by the wind.

The reversal of the flow near Lighthouse Reef as seen in observations (Figs. 2, 6a) can be explained by the eddy calculations. Yet to be explained is the reversal of the flow near Chinchorro Channel (Figs. 7, 10a–d), which seems to occur with or without eddies. Figure 12 shows cross sections near Chinchorro of temperature, salinity and north–south velocity. Salinity variations are relatively small (~0.5 psu) compared to variations in temperature (~4°C), so that density gradients are dominated by temperature gradients. During January warmer surface waters are found near the Mexican coast and colder waters near the bottom, while during April the warmer waters are found offshore near the Chinchorro Island. Therefore, the change in the density gradients across the channel is likely to produce a southward geostrophic flow in January and northward flow during April, as in fact seen in the model (Fig. 12e, f).

While the current model resolution is not sufficient to resolve the details of the lagoon and all the narrow reef channels that connect the lagoon to the open ocean, it can provide the general transports across the reef that influence inflow/outflows to the lagoon; these transports may be important for biological activities. Therefore, the total (vertically integrated) transports at various passages have been calculated and summarized in Fig. 13. With only climatological fields and no eddies (Fig. 13a, b), inflow transports toward the lagoon (blue arrows) are mostly from the north and outflows (red arrows) are toward the east. The only significant change between the two climatologies is the reversal of the transports around the Chinchorro Island, as discussed before. On the other hand, the transport changes due to eddies are very significant, with much stronger transports in January 29 than in April 19. The main reason is that during the first period the strong cyclonic circulation drives southward transports across the length of the lagoon, which exit back eastward through the various passages. During the second period the surface westward flow through the passages is balanced by return flows at deeper layers, so the vertically integrated transports are much weaker. Note that while the 3D WCS model could not resolve

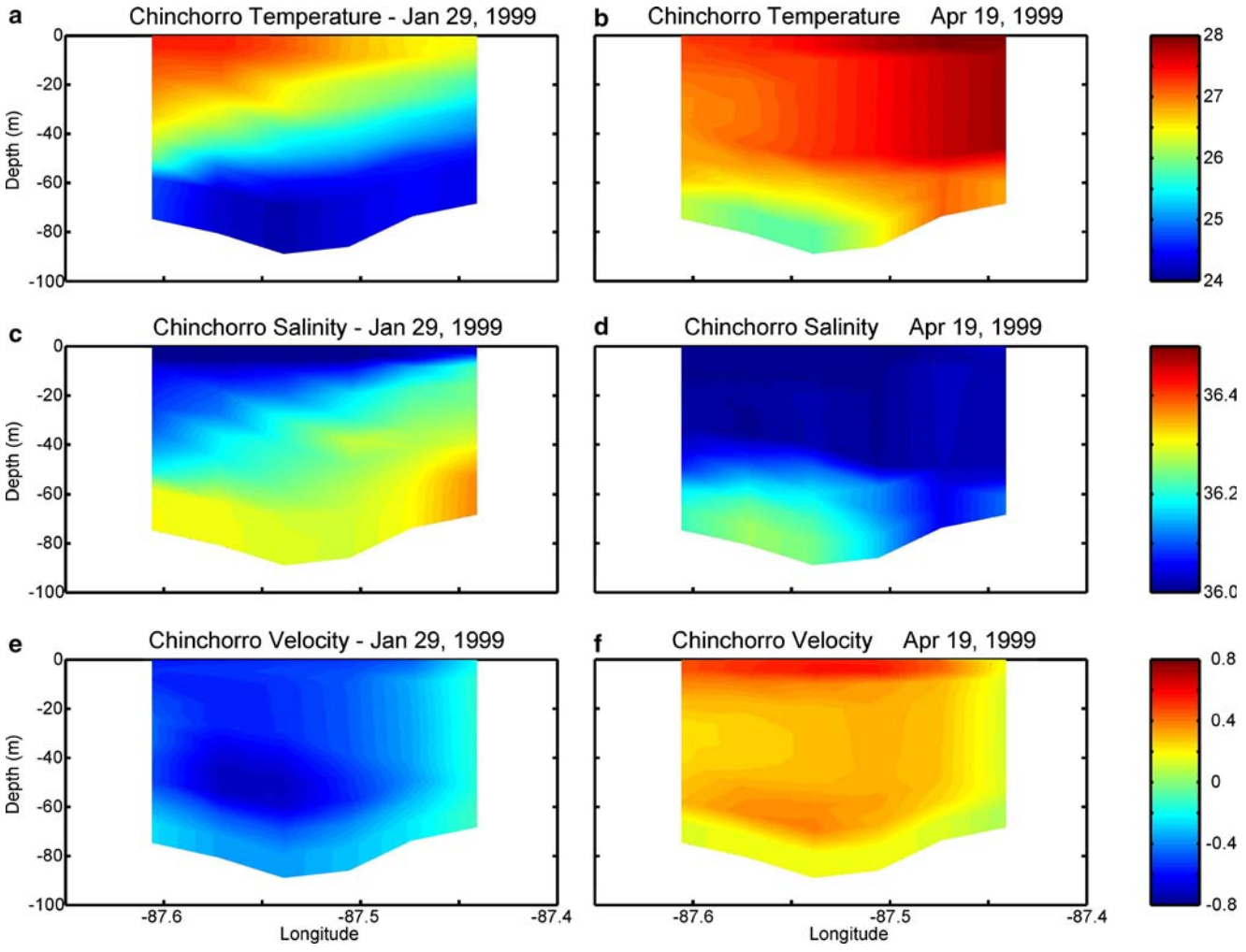

Fig. 12 Cross sections in the Chinchorro channel of temperature (°C), salinity (psu) and V velocity (m/s), from top to bottom, respectively. *Left panels* are for 29 January 1999, *right panels* are for 19 April 1999

most of the channels across the reef as was done in the 2D lagoon model of Thattai (2003) (who had 12 separate channels), the general pattern of inflow transports in the northern channels and outflow transports in the southern channels are generally similar in the 2D and 3D models; both models also indicate that the variation in transports may be larger than the mean transports.

Since transports are difficult to measure directly (may require array of instruments across each passage), we tried to test if sea level observations can be used to estimate variations in transports. Figure 14 shows that in fact, transports and sea level differences are highly correlated. The transports were divided into inflow from the north (between Belize City and Lighthouse Reef) and outflow to the east (between Lighthouse Reef and Puerto Cortes on the Honduras coast), thus only three tidal stations may provide estimates for transport variations across the reef. Note again that in the April 19 eddy case there are almost no net transports (“4” marks in Fig. 14) while in the January 29 eddy case (“3” marks) a total transport of more than 2 Sv enter the lagoon in the north and exit to the east.

4 Discussion and conclusions

A 3D ocean model of the West Caribbean Sea (based on POM) was used to examine the influence that various parameters, such as topography, ocean circulation, climatological wind, climatological density field and Caribbean eddies, may have on the flow along the MBRS. Because of the importance of the MBRS to the local ecology, biology and economy (e.g., the fishing and tourist industries largely depend on the health of the MBRS), better understanding of the variability of the flow along the reef is important. Two types of calculations were done, idealized seasonal calculations to look at the time-dependent nature of the coastal flow and semidiagnostic calculations to identify specific effects such as the existence of eddies near the reef.

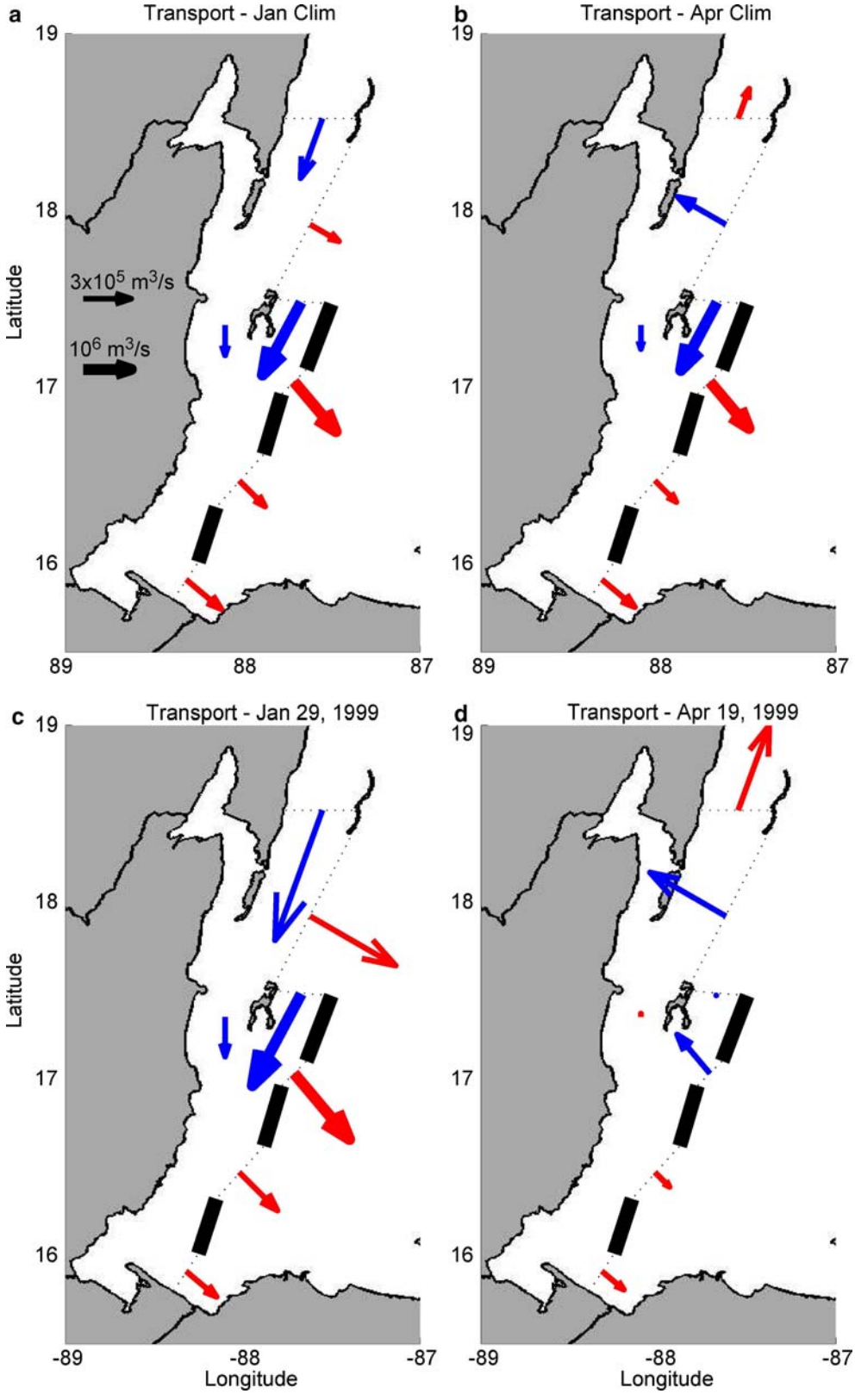

Fig. 13 Total transports across the major passages. *Top panels* are for the climatological cases and *bottom panels* are for the eddies cases; *left panels* are for the January cases and *right panels* are for the April cases. *Blue vectors* represent transports into the Lagoon and *red vectors* represent transports out of the Lagoon (note the different scale for *thin and heavy vectors*)

There are not many direct observations in the GOH and along the coast of Belize (and some contradict with each other, Fig. 2) to give a complete description of the nature of the flow and allow detailed verification of model results. Recent observations are being deployed and will be compared with more realistic model config-

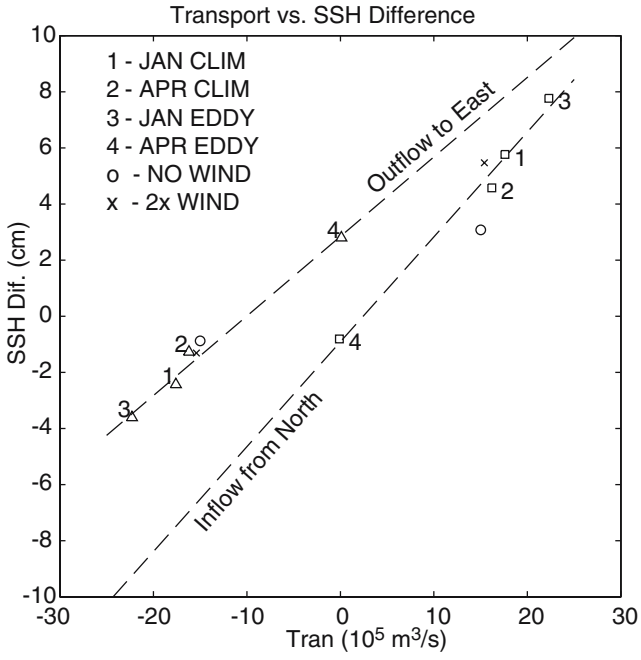

Fig. 14 Total transports across two sections as a function of sea surface height difference across each section. The "inflow from north" section is the sum of all transports (toward the Lagoon) between Lighthouse Reef and Belize City and the "outflow to east" is the sum of all transports between Lighthouse Reef and the coast of Honduras. The different experiments discussed in the paper are indicated by *different marks*

uration in future studies. Nevertheless, the available observations (e.g., drifters, temperature sensors, altimeter) indicate a few interesting findings that have been examined here using a numerical model. In particular, there seem to be strong spatial (Fig. 2) and temporal (Figs. 5d, 6a) variations in the flow along the reef. The seasonal calculations show fluctuations of the CC as it meanders across the topography and produce variations in velocity and temperature along the reef with time scales of a few days to weeks that resemble the observed variations. Model variations are somewhat smaller than observed variations in these scales owing to the fact that except tides and monthly surface climatological wind and temperature, mesoscale and synoptic atmospheric forcings are neglected in the model (including the possibility of eddies propagating into the WCS from the eastern Caribbean Sea). The model indicates the possibility of seasonal reversal of the flow through the Chinchorro Channel; this result was found to be associated with seasonal changes in the density field across the channel and not with changes in the wind.

A simple assimilation scheme was used to obtain 3D density fields that include the signature of Caribbean eddies as inferred from satellite altimeter data. Diagnostic calculations were then used to derive the dynamically adjusted flow associated with the eddy field. Two cases were chosen, the first one with a cyclonic anomaly in the GOH (29 January 1999) and the second

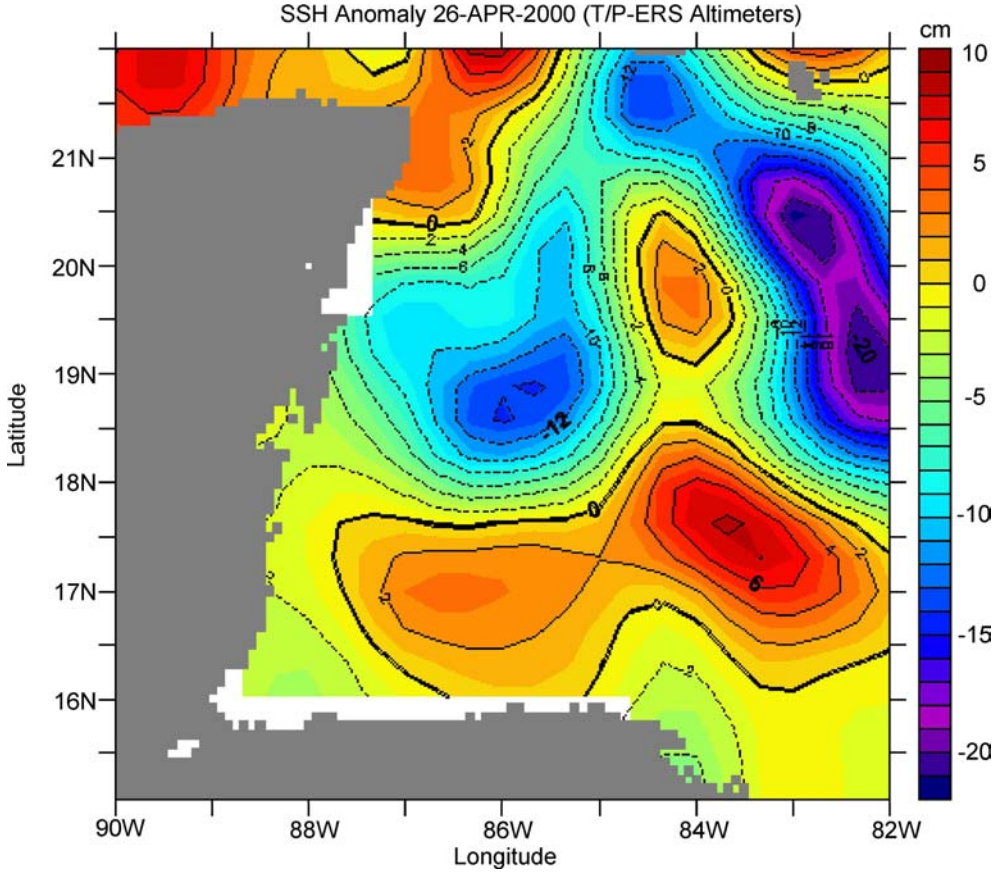

Fig. 15 Observed satellite-derived SSHA (in cm, *red*/*blue* indicates high/low anomaly) for 26 April 2000, obtained from the AVISO altimeter data set (www.aviso.oceanobs.com). This is the time when the drifters in Fig. 2b were launched

one with an anticyclonic anomaly (19 April 1999). The results show a completely different flow field near the MBRS for the two cases. In the first case the CC shifts offshore and the cyclonic circulation in the GOH is intensified so the flow outside the reef is weak, but near the coast flow over the reef and the Meso-American Lagoon is strong and southward. In the second case on the other hand, the CC moves closer to the coast, generating strong northward flow outside the reef, but only weak flows over the lagoon. It is interesting to note that altimeter data and numerical models (Murphy et al. 1999; Ezer and Mellor 2000; Oey et al. 2003) often show that the cyclonic eddies in the GOH originated near the Nicaraguan Rise and are seen propagating westward along the coast of Honduras; these eddies may play an important role in the connectivity processes and associated biological transports along the Caribbean coasts.

Sensitivity model studies show that climatological winds have only small effect on the diagnostic calculations compared with the effect of the density driven circulation (in agreement with the model results of Sheng and Tang 2003). However, effects of synoptic atmospheric events such as storms and hurricanes, as well as effects of rivers runoff in this region (Thattai et al. 2003) may be significant and will require further research.

Can the model results explain the discrepancy between the mean circulation in Fig. 2a (with *southward* flow between Turneffe Islands Atoll and Lighthouse Reefs) and the *northward* propagation of the drifter in Fig. 2b. To answer this questions we looked at the SSH anomaly from the AVISO altimeter data set for the time the drifter was launched, 26 April 2000 (Fig. 15). The eddy field indicates an anticyclonic (positive) anomaly in the GOH in the south and a cyclonic anomaly near the Yucatan peninsula in the north, very similar to the anomalies modeled in the 19 April 1999 case (Fig. 9b). The model calculations in fact show a *northward* velocity between Turneffe and Lighthouse Reefs for this case (Fig. 10d), which is consistent with the drifter behavior of Fig. 2b, but the model results also show a *southward* velocity at the same place for the climatological cases (Fig. 10a, b), which is consistent with the mean flow field of Fig. 2a. Therefore, the model results suggest that the drifters represent the mesoscale eddy field that existed at the time rather than the mean flow field. The observations also provide a qualitative confirmation that the reversal of the flow due to eddies as seen by the model is likely to occur in the real ocean, but further model evaluation is needed with more data.

Variations of transports across the reef and the exchange of water masses between the open ocean and the Meso-American Lagoon may be critical for biological activities such as spawning fish aggregations and reef conservation efforts. However, bottom to surface transports are difficult and expensive to measure directly. Nevertheless, it was shown here that good estimates of transports could be obtained from a few sea level measurements, since sea level differences across passages are correlated with transports when the flow is close to geostrophic balance.

High-resolution basin-scale and regional ocean models such as the various new models that have been developed in recent years for the Intra-America Seas (see Oey et al. 2005, for a review of numerical models of the region) may not resolve the details of the coastal topography, especially in places like the MBRS with shallow lagoons, narrow reef channels and small islands; thus nesting approaches may be needed. However, even the nested MBRS model of Sheng and Tang (2004) is not fine enough to resolve those features and inaccuracy of global topographic data sets near the coast may be a problem (e.g., Fig. 4). Here, a curvilinear orthogonal model grid (with higher resolution near the coast) is used with two hand-fixed topographies, one with the model boundary set along the Belize reef and one that includes a representation of the Meso-American Lagoon across the reef (though not in much detail). The inclusion of the lagoon produces more realistic circulation in places like the Amatique Bay. However, a much higher resolution nested lagoon model, such as the finite element model used by Thattai (2003), is probably needed. It is clear from the results presented here that transports across the reef may change significantly from day to day and from season to season, so that a lagoon model will need to get boundary conditions from larger models, such as that tested here.

Future modeling work with more realistic forcing will be combined with observational campaign (now underway) in collaboration with various scientific and conservational groups from Belize, Mexico and the US.

Acknowledgements The research was supported by funding from the MBRS Project and the Nature Conservancy's Ecosystem Research Program/Mellon Foundation. T.E. is partly supported by grants from the Minerals Management Service (MMS) and the Office for Naval Research (ONR). L. Oey and two reviewees provided useful comments.

References

Andrade CA, Barton ED (2000) Eddy development and motion in the Caribbean Sea. J Geophys Res 105(C11):26191–26201

Appeldoorn RS, Lindeman KC (2003) A Caribbean-wide survey of marine reserves: spatial coverage and attributes of effectiveness. Gulf Caribbean Res 14(2):139–154

Armstrong BN (2005) Currents along the Mesoamerican Reef, Western Caribbean. Marine Science Program Thesis, University of South Carolina, 32 pp

Aronson RB, Precht WF, Toscano MA, Koltes KH (2002) The 1998 bleaching event and its aftermath on a coral reef in Belize. Mar Biol 141: 435–447

Blumberg AF, Mellor GL (1987) A description of a three-dimensional coastal ocean circulation model. In: Heaps NS (eds) Three-dimensional coastal ocean models, vol 4. American Geophysical Union, Washington, DC, pp 1–16

Brucks JT (1971) Currents of the Caribbean and adjacent regions as deduced from drift-bottle studies. Bull Mar Sci 21(2):455–465

Bunge L, Ochoa J, Badan A, Candela J, Sheinbaum J (2002) Deep flows in the Yucatan Channel and their relation to changes in the Loop Current extension. J Geophys Res 107(C12). DOI 10.1029/2001JC001256

Burke L, Maidens J (2004) Reefs at risk in the Caribbean. World Resources Institute, Washington, D.C., pp 80

Candela J, Tanahara S, Crepon M, Barnier B, Sheinbaum J (2003) Yucatan Channel flow: observations versus CLIPPER ATL6 and MERCATOR PAM models. J Geophys Res 108(C12). DOI 10.1029/2003JC001961

Carton JA, Chao Y (1999) Caribbean Sea eddies inferred from TOPEX/POSEIDON altimetry and a 1/6o Atlantic Ocean model simulation. J Geophys Res 104(C4):7743–7752. DOI 10.1029/1998JC900081

Chen P, Mellor GL (1999) Determination of tidal boundary forcing using tide station data. In: Mooers CNK (eds) Coastal ocean prediction, coastal and estuarine studies 56. American Geophysical Union, Washington, DC, pp 329–351

Craig AK (1966) Geography of fishing in British Honduras and adjacent coastal waters. Louisiana State University Press, 143 pp

da Silveira IC, Calado AL, Castro BM, Cirano M, Lima JMA, Mascarenhas ADS (2004) On the baroclinic structure of the Brazil Current–Intermediate Western Boundary Current system at 22°–23°S. Geophys Res Let 31(L14308). DOI 10.1029/2004GL020036

Ducet N, Le Tron PY, Reverdin G (2000) Global high-resolution mapping of ocean circulation from TOPEX/Poseidon and ERS−1 and −2. J Geophys Res 105(C8):19477–19498. DOI 10.1029/2000JC900063

Ezer T, Mellor GL (1994a) Diagnostic and prognostic calculations of the North Atlantic circulation and sea level using a sigma coordinate ocean model. J Geophys Res 94:14159–14171

Ezer T, Mellor GL (1994b) Continuous assimilation of Geosat altimeter data into a three-dimensional primitive equation Gulf Stream model. J Phys Oceanogr 24:832–847

Ezer T, Mellor GL (1997) Data assimilation experiments in the Gulf Stream region: how useful are satellite-derived surface data for nowcasting the subsurface fields? J Atmos Ocean Tech 16(6):1379–1391

Ezer T, Mellor GL (2000) Sensitivity studies with the North Atlantic sigma coordinate Princeton Ocean Model. Dyn Atmos Ocean 32:185–208

Ezer T, Arango H, Shchepetkin AF (2002) Developments in terrain-following ocean models: intercomparisons of numerical aspects. Ocean Mod 4:249–267

Ezer T, Oey L-Y, Lee H-C, Sturges W (2003) The variability of currents in the Yucatan Channel: analysis of results from a numerical ocean model. J Geophys Res 108(C1):3012. DOI 10.1029/2002JC001509

Fratantoni DM (2001) North Atlantic surface circulation during the 1990s observed with satellite-tracked drifters. J Geophys Res 106(C10):22067–22093. DOI 10.1029/2000JC000730

Gardner TA, Cote IM, Gill JA, Grant A, Watkinson AR (2003) Long-term region-wide declines in Caribbean corals. Science 301:958–960

Gibson J, McField M Heyman W, Wells S, Carter J, Sedberry G (2004) Belize's evolving system of marine reserves. In: Sobel J, Dahlgren C (eds) Marine reserves: a guide to science, design and use. The Ocean Conservancy, Washington, D.C., pp 287–315

Gordon AL (1967) Circulation of the Caribbean Sea. J Geophys Res 72(24):6207–6223

Heyman WD, Kjerfve B (2000) The Gulf of Honduras. In: Seeliger U, Kjerfve B (eds) Coastal marine ecosystems of Latin America. Ecological studies, vol 144. Springer, Berlin, Heidelberg, New York

Heyman WD, Graham RT, Kjerfve B, Johannes RE (2001) Whale sharks Rhincodon typus aggregate to feed on fish spawn in Belize. Mar Ecol Prog Ser 215:275–282

Heyman WD, Kjerfve B, Rhodes KL, Grahm RT, Garbutt L (2005) Cubera snapper spawning aggregation on the Belize Barrier Reef. J Fish Biol 66(5):1–19

Kjerfve B (1981) Tides of the Caribbean Sea. J Geophys Res 86(C5):4243–4247

Kinder TH (1983) Shallow currents in the Caribbean Sea and Gulf of Mexico as observed with satellite-tracked drifters. Bull Mar Sci 33:239–246

Mellor GL, Blumberg AF (1985) Modeling vertical and horizontal diffusivities with the sigma coordinate system. Mon Wea Rev 113:1380–1383

Mellor GL, Ezer T (1991) A Gulf stream model and an altimetry assimilation scheme. J Geophys Res 96(C5):8779–8795

Mellor GL, Ezer T, Oey L-Y (1994) The pressure gradient conundrum of sigma coordinate ocean models. J Atmos Ocean Tech 11:1126–1134

Mellor GL, Oey L-Y, Ezer T (1998) Sigma coordinate pressure gradient errors and the seamount problem. . J Atmos Ocean Tech 15:1122–1131

Mellor GL, Yamada T (1982) Development of a turbulent closure model for geophysical fluid problems. Rev Geophys 20:851–875

Molinari RL, Spillane M, Brooks I, Atwood D, Duckett C (1981) Surface currents in the Caribbean Sea as deduced from Lagrangian observations. J Geophys Res 86(C7):6537–6542

Morey SL, Martin PJ, O'Brien JJ, Wallcraft AA, Zavala-Hidalgo J (2003) Export pathways for river discharged fresh water in the northern Gulf of Mexico. J Geophys Res 108(C10):3303. DOI 10.1029/2002JC001764

Murphy SJ, Hulburt HE, O'Brien JJ (1999) The connectivity of eddy variability in the Caribbean Sea, the Gulf of Mexico, and the Atlantic Ocean. J Geophys Res 104(C1):1431–1453. DOI 10.1029/1998JC900010

Ochoa J, Candela J, Badan A, Sheinbaum J (2005) Ageostrophic fluctuations in the Cozumel Channel. J Geophys Res 110(C2). DOI 10.1029/2004JC002408

Ochoa J, Sheinbaum J, Baden A, Candela J, Wilson D (2001) Geostrophy via potential vorticity inversion in the Yucatan Channel. J Mar Res 59:725–747

Oey L-Y, Lee H-C, Schmitz WJ (2003) Effects of winds and Caribbean eddies on the frequency of Loop Current eddy shedding: a numerical model study. J Geophys Res 108(C10):3324. DOI 10.1029/2002JC001698

Oey L-Y, Ezer T, Lee H-C (2005) Loop current, rings and related circulation in the Gulf of Mexico: a review of numerical models and future challenges. In: Sturges W, Fernandez AL (eds) Ocean circulation in the Gulf of Mexico. Geophys Monograph Ser, American Geophysical Union, Washington, D.C. (in press)

Ray R (1999) A global ocean tide model from Topex/Poseidon altimetry: GOT99.2, NASA Tech Memo 209478, 58 pp

Roberts CM, McClean J, Vernon JEN, Howkins JP, Allen GR,McAllister DE, Mittermeier CG, Schueler PW, Spalding M, Wells F, Vynne C, Werner TB (2002) Marine biodiversity hotspots and conservation priorities for tropical reefs. Science 295:1280–1284

Romanou A, Chassignet EP, Sturges W (2004) The Gulf of Mexico circulation within a high resolution numerical simulation of the North Atlantic Ocean. J Geophys Res 109:CO1003. DOI 10.1029/2003CJ001770

Sala E, Ballesteros E, Starr RM (2001) Rapid decline of Nassau grouper spawning aggregations in Belize: fishery management and conservation needs. Fisheries 26:23–30

Sheng J, Tang L (2003) A numerical study of circulation in the western Caribbean Sea. J Phys Oceanogr 33:2049–2069

Sheng J, Tang L (2004) A two-way nested-grid ocean circulation model for the Meso-American Barrier Reef System. Ocean Dyn 54:232–242

Smagorinsky J, Manabe S, Holloway JL (1965) Numerical results from a nine-level general circulation model of the atmosphere. Mon Wea Rev 93:727–768

Sou T, Holloway G, Eby M (1996) Effects of topographic stress on Caribbean Sea circulation. J Geophys Res 101(C7):16449–16453

Teague WJ, Carron MJ, Hogan PJ (1990) A comparison between the generalized digital environmental model and Levitus climatologies. J Geophys Res 95(C5):7167–7183

Thattai DV (2003) Modeling the hydrometeorology and circulation in the Gulf of Honduras and the Mesoamerican Lagoon, western Caribbean. PhD Dissertation, Department of Geological Sciences, University of South Carolina, 122 pp

Thattai DV, Kjerfve B, Heyman WD (2003) Hydrometeorology and variability of water discharge and sediment load in the inner Gulf of Honduras, western Caribbean. J Hydrometeor 4:985–995

Vidal VMV, Vidal FV, Perez-Molero JM (1992) Collision of a Loop Current anticyclonic ring against the continental slope of the western Gulf of Mexico. J Geophys Res 97(C2):2155–2172

Wang D-P, Oey L-Y, Ezer T, Hamilton P (2003) Near-surface currents in DeSoto Canyon (1997–99): comparison of current meters, satellite observation, and model simulation. J Phys Oceanogr 33:313–326

Wang H, Yuan Y, Guan W, Lou R, Wang K (2004) Circulation in the South China Sea during summer 2000 as obtained from observations and a generalized topography-following ocean model. J Geophys Res 109:C07007. DOI 10.1029/2003JC002134

Wong LA, Chen JC, Xue H, Dong LX, Su JL, Heinke G (2003) A model study of the circulation in the Pearl River Estuary (PRE) and its adjacent coastal waters: 1. Simulations and comparison with observations. J Geophys Res 108(C5):3156. DOI 10.1029/2002JC001451